doi:10.1093/brain/awx286 BRAIN 2017: 140; 3153–3165 | 3153

BRAIN
A JOURNAL OF NEUROLOGY

Induced cortical responses require developmental sensory experience

Prasandhya Astagiri Yusuf,[1] Peter Hubka,[1] Jochen Tillein[1,2] and Andrej Kral[1,3]

Sensory areas of the cerebral cortex integrate the sensory inputs with the ongoing activity. We studied how complete absence of auditory experience affects this process in a higher mammal model of complete sensory deprivation, the congenitally deaf cat. Cortical responses were elicited by intracochlear electric stimulation using cochlear implants in adult hearing controls and deaf cats. Additionally, in hearing controls, acoustic stimuli were used to assess the effect of stimulus mode (electric versus acoustic) on the cortical responses. We evaluated time-frequency representations of local field potential recorded simultaneously in the primary auditory cortex and a higher-order area, the posterior auditory field, known to be differentially involved in cross-modal (visual) reorganization in deaf cats. The results showed the appearance of evoked (phase-locked) responses at early latencies (<100 ms post-stimulus) and more abundant induced (non-phase-locked) responses at later latencies (>150 ms post-stimulus). In deaf cats, substantially reduced induced responses were observed in overall power as well as duration in both investigated fields. Additionally, a reduction of ongoing alpha band activity was found in the posterior auditory field (but not in primary auditory cortex) of deaf cats. The present study demonstrates that induced activity requires developmental experience and suggests that higher-order areas involved in the cross-modal reorganization show more auditory deficits than primary areas.

1 Institute of AudioNeuroTechnology and Department of Experimental Otology, ENT Clinics, Hannover Medical School, Germany
2 ENT Clinics, J. W. Goethe University, Frankfurt am Main, Germany
3 School of Behavioral and Brain Sciences, The University of Texas at Dallas, USA

Correspondence to: Andrej Kral, MD, PhD
Institute of AudioNeuroTechnology,
Stadtfelddamm 34,
D-30625 Hannover,
Germany
E-mail: kral.andrej@mh-hannover.de

Keywords: congenital deafness; sensory deprivation; cortical oscillations; secondary field; cochlear implant

Abbreviations: A1 = primary auditory cortex; b-LFP = bipolar derivation LFP; CDC = congenitally deaf (white) cat; LFP = local field potential; PAF = posterior auditory field; PLF = phase-locking factor; TFR = time-frequency representation

Introduction

Sensory perception results from interaction between sensory input and ongoing cortical activity (Steriade, 1993; Castro-Alamancos, 2004; Gilbert and Sigman, 2007; Lakatos *et al*., 2007; Poulet and Petersen, 2008), which contains information on the internal model of the environment and the subject (Berkes *et al*., 2011; see also Wolpert *et al*., 1995; Ito, 2008), i.e. information on subjective meaning and context. Neuronal oscillations or oscillatory transients (referred together as 'oscillatory activity' here) are involved in such interactions in different brain regions (Lakatos *et al*., 2007; Buzsáki and Wang, 2012; Giraud and Poeppel, 2012). Oscillatory activity has been, among other functions, also related to stimulus detection and stimulus selection (Fiebelkorn *et al*., 2013; Mercier *et al*.,

Received May 2, 2017. Revised August 1, 2017. Accepted September 12, 2017.
© The Authors (2017). Published by Oxford University Press on behalf of the Guarantors of Brain.
This is an Open Access article distributed under the terms of the Creative Commons Attribution Non-Commercial License (http://creativecommons.org/licenses/by-nc/4.0/), which permits non-commercial re-use, distribution, and reproduction in any medium, provided the original work is properly cited. For commercial re-use, please contact journals.permissions@oup.com

2015; Lakatos *et al*., 2016; van de Nieuwenhuijzen *et al*., 2016), auditory stimulus familiarity and choice (Handa *et al*., 2017), sound perception (Ross *et al*., 2017), listening effort (Dimitrijevic *et al*., 2017) and auditory attention (Wöstmann *et al*., 2017), auditory streaming (Riecke *et al*., 2015), and auditory decision tasks (Strauß *et al*., 2014). Of clinical importance is that oscillatory activity is tightly related to language physiology (Shahin *et al*., 2009; Lewis *et al*., 2015*a*; Dimitrijevic *et al*., 2017) and that many forms of language pathology are accompanied by abnormal oscillatory activity (Gandal *et al*., 2010; Goswami, 2011, 2014; Heim *et al*., 2011; Edgar *et al*., 2015; Murphy and Benítez-Burraco, 2017). This is particularly interesting for hearing restoration with cochlear implant that aims to allow speech comprehension in deaf subjects.

Event-related oscillatory activity consists of evoked and induced responses (Tallon-Baudry *et al*., 1996; Donner and Siegel, 2011; Chen *et al*., 2012). The evoked response reflects phase-locked activity and mirrors primarily activation of thalamo-cortical loops processing sensory (bottom-up) input (Arieli *et al*., 1996; Lakatos *et al*., 2009). The induced response, on the other hand, varies from trial to trial, most likely reflecting the interaction between the incoming sensory information and other active inputs into the same neurons. Consequently, the induced response reflects integration of sensory input and ongoing activity (David *et al*., 2006), including cortico-cortical feedback information (Pfurtscheller and Lopes da Silva, 1999; Morillon *et al*., 2015) conveying the semantic content of the stimulus (Fründ *et al*., 2008). The induced response may thus represent top-down influences on bottom-up processing (Tallon-Baudry and Bertrand, 1999; Alain *et al*., 2001; McMains and Kastner, 2011; Chen *et al*., 2012).

The effect of developmental sensory experience on the integration of sensory input into ongoing cortical activity has rarely been investigated. Representation of sensory information critically depends on experience-dependent fine-tuning of cortical networks during development (Alain *et al*., 2001; Gilbert and Sigman, 2007; Kral and Eggermont, 2007), including the networks in the auditory cortex (Kral *et al*., 2005, 2017; Barone *et al*., 2013; Tillein *et al*., 2016). Defining the relation of oscillatory activity and sensory experience could help to understand pathophysiological background of neurodevelopmental disorders and lead to an objective clinical measure for diagnosis and monitoring of the rehabilitation process (e.g. following neurosensory restoration and training procedures).

We used congenitally deaf (white) cats (CDCs) as a higher mammal model of complete and congenital sensory deprivation (Heid *et al*., 1998; Kral *et al*., 2006). We compared evoked and induced activity recorded simultaneously with multielectrode arrays in the primary auditory cortex (A1) and higher-order posterior auditory field (PAF) under acoustic and electric stimulation (using cochlear implants). A1 and PAF are known to be differentially involved in cross-modal (visual) reorganization in CDCs (Kral *et al*., 2003; Lomber *et al*., 2010), allowing comparison of a field that serves a cross-modal (visual) function (PAF) to another one where such cross-modal function has not been observed (A1). The outcomes provide evidence of compromised induced responses in both investigated fields and higher extent of functional deficits in the higher-order auditory field in congenital deafness. Selective impairment of induced (non-phase-locked) responses could be thus used as an indicator of compromised ability of cerebral cortex to integrate incoming sensory information.

Materials and methods

Animals

Fifteen adult cats, 10 normal hearing controls, and five CDCs, were used. The CDCs were selected from a colony of deaf white cats (Kral and Lomber, 2015) using early screening of hearing status with acoustically-evoked brainstem evoked responses up to 120 dB sound pressure level (SPL) (Heid *et al*., 1998). The animals' hearing status was additionally confirmed at the beginning of the acute experiments. From the 10 normal controls, four were stimulated only acoustically, two were first stimulated acoustically and afterward stimulated electrically using a cochlear implant, and the last four were stimulated exclusively using a cochlear implant. This resulted in a sample of six electrically- and six acoustically-stimulated datasets.

To prevent electrophonic responses (electrical stimulation of hair cells) in the electrically-stimulated hearing animals, the hair cells (present in controls but absent in CDCs) had to be destroyed pharmacologically by intracochlear application of neomycin into the scala tympani (Hartmann *et al*., 1984). The adjective 'hearing' thus does not refer to the functional state of the cochlea during the experiment, but to the developmental and functional state of the central auditory system that has developed under the normal cochlear function until the moment of the acute experiment.

The experiments were approved by the local state authorities and were performed in compliance with the Guidelines of the European Community for the care and use of laboratory animals (EUVD 86/609/EEC) and the German Animal Welfare Act (TierSchG).

Experimental procedures

All animals were premedicated with 0.25 mg atropine i.p. and initially anaesthetized with ketamine hydrochloride (24.5 mg/kg, Ketavet®, Parker-Davis) and propionyl promazine phosphate (2.1 mg/kg, Combelen, Bayer). They were then tracheotomized and artificially ventilated with 50% O_2 and 50% N_2O, with the addition of 0.2–1.5% concentration of isoflurane (Lilly) to maintain a controlled depth of anaesthesia (Kral *et al*., 1999). Care was taken to preserve light anaesthesia levels by keeping suppression index values within the range of 1 to 3 (Land *et al*., 2012).

The animal's head was fixed in a stereotactic frame (Horsley-Clarke). Both bullae and ear canals were subsequently exposed. To record evoked auditory brainstem responses, a small trephination was drilled at the vertex of the skull and a silver-ball electrode (diameter 1 mm) was attached

epidurally. The indifferent electrode used for the recordings was inserted medially into the neck muscles.

Hearing status was verified using auditory brainstem evoked responses (ABRs) with condensation clicks applied through a calibrated speaker (DT48, Bayer Dynamics) at levels up to 120 dB SPL. For electrical stimulation, controls and CDCs were implanted with a cochlear implant inserted via the round window. Electrically evoked auditory brainstem response (E-ABR) to single biphasic pulses was recorded and the lowest current levels evoking a brainstem response (E-ABR threshold currents) were determined.

In A1, recordings were at positions showing the largest surface local field potentials (LFPs) determined in surface mapping ('hot spots'; for details see Kral *et al*., 2009, 2013). A single-shank multi-electrode array (NeuroNexus, single shank, 16 contacts, spacing 150 µm, 177 μm^2 contact area, electrode array length 2400 µm, impedance ~1–2 MΩ) was used to penetrate A1 perpendicularly to the cortical surface to 2400 µm depth. A second array was used to map and register activity in field PAF (Supplementary Fig. 1). In PAF, the penetration was only possible parallel to the cortical surface (Fig. 1). PAF penetrations were performed in two insertion steps: first we penetrated to 5000 µm depth, performed the recordings, and subsequently retracted the probe to 2500 µm depth (Fig. 1B). At least one PAF penetration in each animal was marked by a fluorescent dye (DiI, 1,1′-dioctadecyl-3,3,3',3'-tetramethylindocarbocyanine perchlorate; Invitrogen) to allow histological reconstruction of the penetration track. For all recordings, the cortex was stabilized by a modified Davies chamber (Tillein *et al*., 2010).

Stimulation and recording

The contralateral ears were electrically stimulated by three biphasic electric charge-balanced pulses (200 µs/phase) presented through cochlear implants or acoustically stimulated by three condensation clicks (50 µs duration) presented through loudspeakers (repetition rate 500 pps, stimulus duration 4.4 ms). Stimulus presentation rate was 1/1537 ms with 30 stimulus repetitions. Stimulation level was increased in 10 dB (acoustic) or 1–2 dB (electric) steps. Stimulation intensities were from at least 10 dB (acoustic) or 1 dB (electric) below threshold to at least 40 dB (acoustic) or 9 dB (electric) above acoustic and electric ABR-threshold.

For recording, signals were amplified by a 64-channel Cheetah amplifier (Neuralynx) with a gain of 5000 and open filters (1–9000 Hz), fed to a multifunctional data acquisition card (NI PCIe 6259, National Instruments), 16-bit A/D converted at sampling rate of 25 kHz per channel and stored on a computer.

Data analysis in time domain

Offline data analyses were performed using the FieldTrip toolbox (Oostenveld *et al*., 2011) and custom-made Matlab scripts (Matlab, Mathworks). Recordings with technical artefacts or periods with repeated spontaneous bursting were excluded from the analysis.

Multiunit activity was determined offline using high-pass filtering (elliptic IIR filter, second-order, and high-pass edge frequency of 400 Hz), electrical stimulus artefacts were blanked

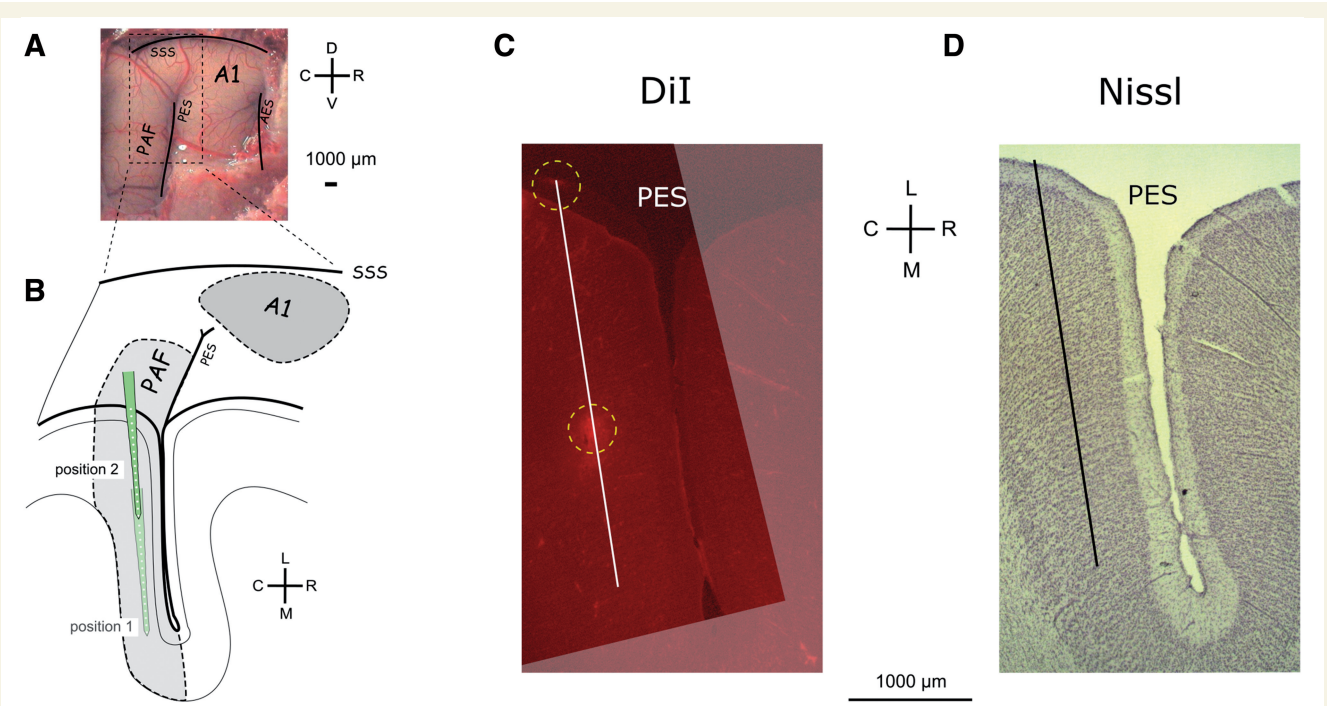

Figure 1 Recording positions in the posterior auditory field. (**A**) Photograph of the cortex after trephination revealing the sulcal patterns in the cat. (**B**) Schematic illustration of the penetrations in PAF in their relative position to the posterior ectosylvian sulcus. With two recording depths, each penetration includes 32 recording sites in total. A dense mapping of the field allowed capturing the auditory responses in each animal. (**C**) Reconstruction of a microelectrode penetration stained with a fluorescence dye from a histological section in a deaf cat. The DiI-stained images were stacked and aligned to reconstruct the penetration. (**D**) Nissl staining from the same section as in **C** demonstrates recordings in supragranular layers. AES = anterior ectosylvian sulcus; C = caudal; D = dorsal; L = lateral; M = medial; PES = posterior ectosylvian sulcus; R = rostral; SSS = suprasylvian sulcus; V = ventral.

and linearly interpolated (0–6 ms post-stimulus). Zero-phase digital filtering was performed to avoid latency shifts. Unit activity was quantified by an automatic thresholding procedure for spike detection (Quiroga *et al*., 2004), and the peristimulus time histogram (PSTH) was constructed by 1 ms binning of unit responses from all repetitions. We used this unit activity to determine and compare the distribution of the responding channels within the penetration tracks in PAF (Supplementary Fig. 1B). A channel was considered responding if the peak of post-stimulus (0–50 ms) activity exceeded mean + 4 times standard deviation (SD) of the prestimulus baseline (corresponding to $P < 0.00006$).

LFP signals were first resampled (1 kHz sampling rate) and were baseline corrected in the time domain (to eliminate overall baseline drift and to minimize edge artefacts in time-frequency computation) (Herrmann *et al*., 2014). Afterwards, discrete Fourier transform (DFT) filter at 50 and 100 Hz was used to eliminate possible power line artefact. To eliminate volume conduction and the common reference problem (Bastos and Schoffelen, 2016), LFPs in neighbouring channels were subtracted to compute 'bipolar derivation LFPs' (denoted as b-LFP). We used two-tailed Wilcoxon rank-sum tests for all statistical group and field comparisons based on PSTHs and LFPs.

Time-frequency analysis of bipolar derivation local field potentials

Time-frequency representation (TFR) was calculated using complex wavelet transformation (Morlet wavelets, m = 6, 1 ms steps, frequencies 5–119 Hz with 2 Hz linear steps). Time-frequency regions affected by the edge (border) artefacts were excluded from the analysis.

Phase-locking factor (PLF, Tallon-Baudry *et al*., 1996) was computed prior to DFT filter. The complex TFRs for each trial were first normalized (vector length = 1), summed (vector addition) over trials, then the absolute value was taken. We used the PLF critical value as a statistical threshold (Cohen, 2014):

$$PLF_{crit} = \sqrt{\frac{-ln(P)}{n}} \quad (1)$$

where P denotes P-value and n number of trials. With $n = 30$ and $P = 0.01$, consequently, PLF_{crit} for our set-up was 0.3918.

Channels were considered responding if the early-latency PLF value (0–100 ms post-stimulus) exceeded mean + 4 times SD of baseline activity in any consecutive 20 ms time window at any frequency. Site threshold (~0 dB) was determined as the lowest stimulation level at which a significant PLF response could be detected at any frequency within the TFR. Subsequently, stimulation levels were aligned relative to site threshold into [<0, 0, 1, 3, 6, 9] dB (electric) and [<0, 0, 10, 20, 40, 60] dB (acoustic) and level functions (Supplementary Fig. 4) were constructed using the maximum early-latency PLF value, for each level. Here, PLF value is advantageous across group comparison since it is intrinsically normalized and less affected by spontaneous activity than spectral amplitude. Only recording sites that were responding in a minimum of two subsequent stimulus levels were included. Two-tailed Wilcoxon rank-sum test with Bonferroni correction was used for statistical comparisons.

To compute TFR power, the complex TFRs for each trial were squared and averaged throughout all trials. We used median averaging to minimize outlier effects (Griffiths *et al*., 2010; Cohen, 2014; Lewis *et al*., 2015*b*). The total power TFR was computed from the TFRs of the single-trial b-LFPs. Induced power was determined by subtracting the time-average b-LFP from each trial before TFR computation (Cohen, 2014). Subsequently, we normalized both total and induced TFRs in dB scale relative to the baseline period (−400 to −100 ms prestimulus). Additionally, the (baseline-normalized) evoked TFR was obtained by subtracting the baseline-normalized induced TFR from the baseline-normalized total TFR (Donner and Siegel, 2011; Cohen, 2014). The TFR maps computed using PLF and using evoked TFR were very similar (Supplementary Fig. 3). We chose evoked TFR as a representation of phase-locked activation and induced TFR as a representation of non-phase locked activity. This allowed expressing them in the same unit (dB relative to baseline) and thus directly comparing phase-locked and non-phase-locked responses.

Subsequently, we reported comparisons at 6 dB above site threshold. TFRs from responding channels within each experimental group and field were pooled to compute the corresponding grand mean. Statistical time-frequency differences between groups were performed using non-parametric cluster-based permutation test (Maris and Oostenveld, 2007) with 1000 random permutations under the null hypothesis (cluster α threshold 1%, two-tail significant α-value = 0.5%).

The power spectra of ongoing activity were computed from the subthreshold b-LFPs. Multitaper analysis with three tapers in frequency from 5–120 Hz with 2.5 Hz steps was used. Statistical comparisons were performed using two-tailed Wilcoxon rank-sum test, with false detection rate correction ($q < 0.001$) (Benjamini and Yekutieli, 2001). The relative differences were computed by subtracting the median of two groups divided by the sum medians of the two groups.

$$RelativeDifference = \frac{A - B}{A + B} * 100\ [\%] \quad (2)$$

Results

Responses differ between primary auditory cortex and posterior auditory field

A1 and PAF are anatomically and functionally distinct areas delimited by the sulcal pattern (Fig. 1A). Recording positions in A1 were determined functionally by selecting the most responsive region using surface mapping (Kral *et al*., 2009). Since PAF is partly hidden in the sulcus, instead of surface mapping, this field has been densely penetrated throughout its whole dorsoventral extent (Fig. 1 and Supplementary Fig. 1). Reconstructions of the electrode insertion sites using DiI combined with Nissl staining confirmed that recordings were taken in supragranular layers

of PAF (Fig. 1C and D). The auditory unit responses in PAF covered the whole caudal bank of the posterior ectosylvian sulcus down to its deepest point in all groups (Supplementary Fig. 1B).

The (unipolar) LFPs in A1 and PAF (Fig. 2A) had different morphology, confirming their source in a primary and secondary cortical field (Eggermont, 1992; Fallon *et al.*, 2014). The A1 response was the same as previously described for electric stimulation (Kral *et al.*, 2005, 2009). For both electrically-stimulated controls and CDCs, the PAF responses had smaller averaged amplitudes (Table 1, $P < 0.001$, rank-sum test) and longer latencies (Fig. 2D and Table 1, $P < 0.001$, rank-sum test).

First spatial (bipolar) derivation along the shank of the electrode was subsequently performed to eliminate the contribution of the reference electrode and far-field sources (denoted as b-LFP, Fig. 2B). There were no significant amplitude differences between A1 and PAF in electrically-stimulated controls but smaller b-LFPs in field PAF in CDCs (Table 1, $P = 0.689$ and $P < 0.001$, respectively, rank-sum test). PAF showed longer latencies than A1 in both groups of animals (Fig. 2E and Table 1, $P < 0.001$, rank-sum test).

In unit activity (Fig. 2C), there were stronger responses recorded in A1 than PAF in both electrically-stimulated controls and CDCs ($P < 0.01$ and $P < 0.001$, respectively,

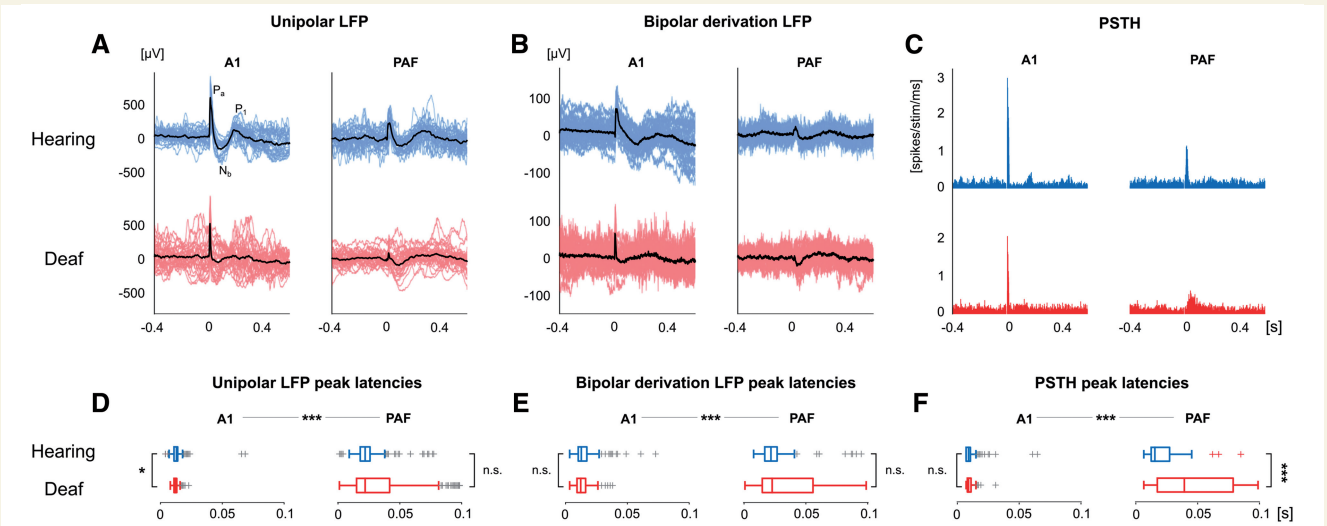

Figure 2 Examples of local field potentials and unit responses. (**A**) Unipolar LFP examples for electrically-stimulated hearing controls (blue) and deaf animals (red) in field A1 and the higher-order field PAF. Individual trials and their average are shown in colour and black, respectively, with P_a, N_b, P_l components. (**B**) Same as **A** for bipolar derivation (b-LFP) response—eliminating the influence of the common reference and minimizing volume conduction. (**C**) Same as **A** for individual multiunit responses plotted as peristimulus time histograms (PSTHs). (**D**) The statistical distribution of peak-latencies for unipolar LFPs. (**E**) Same as **D** for b-LFPs. (**F**) Same as **D** for multi-unit activity peak-latencies. All responses were elicited by intracochlear electrical stimulation at the intensity of 6 dB above the site-threshold. **D–F** show significantly longer peak latencies in PAF than in A1 ($P < 0.001$), two-tailed Wilcoxon rank-sum test. *$P < 0.05$; ***$P < 0.001$; n.s. = not significant.

Table 1 Amplitudes and latencies of LFPs and unit activity in A1 and PAF of hearing controls and CDCs

	Electrically-stimulated hearing controls			Congenitally deaf cats		
	A1	PAF	*P*-value	A1	PAF	*P*-value
Unipolar LFP						
Absolute maxima (μV)	276.41 ± 240.17	197.58 ± 206.39	<0.001	328.96 ± 179.11	72.38 ± 35.37	<0.001
Peak latencies (ms)	13.70 ± 6.68	23.99 ± 12.34	<0.001	12.61 ± 2.72	33.33 ± 27.53	<0.001
Bipolar derivation LFP						
Absolute maxima (μV)	77.83 ± 100.40	89.88 ± 165.10	0.689	86.53 ± 75.66	37.48 ± 21.85	<0.001
Peak latencies (ms)	14.84 ± 8.48	23.96 ± 14.12	<0.001	13.32 ± 5.77	36.80 ± 30.57	<0.001
Unit activity						
Spike rate (sp/stim/ms)	1.189 ± 0.758	0.928 ± 0.550	<0.01	1.172 ± 0.656	0.406 ± 0.181	<0.001
Peak latencies (ms)	9.01 ± 3.26	18.99 ± 9.73	<0.001	9.19 ± 3.28	23.39 ± 12.97	<0.001

sp = spike; stim = stimulus.
Values: mean ± standard deviation; statistics: non-parametric two-tailed Wilcoxon rank-sum test.

rank-sum test) along with longer latencies in PAF than A1 (Fig. 2F, $P < 0.001$, rank-sum test, Table 1).

Altogether, these results confirmed the expected difference between A1 and PAF: partly smaller response amplitude and consistently longer latencies in the secondary field PAF. Furthermore, PAF responses were distributed along a longer time window (for acoustically-stimulated controls, see Supplementary Fig. 2). Except for larger range of latencies and smaller amplitudes in PAF, deafness did not systematically affect LFP properties. In what follows, only b-LFPs were analysed further.

Evoked and induced time-frequency representations of hearing controls

Subsequently, b-LFPs were decomposed into individual frequencies using wavelet analysis. We analysed total, evoked and induced TFRs (see 'Materials and methods' section). Electrically-stimulated controls showed activity from the stimulus onset until the end of the recording (Fig. 3A and Supplementary Fig. 3). As expected, the evoked response part (Fig. 3B) dominated the 'early' time window (0 to 100 ms after stimulus onset). The induced response (Fig. 3C) was observed at the early but even more at the 'late' time window (150 to 500 ms post-stimulus). In PAF the total response had less power (Fig. 3D) but showed similar properties of evoked and induced activity as in A1 (Fig. 3E and F). The evoked response is thus dominating the early while the induced activity the late response.

Activity was further classified into alpha (7–15 Hz), beta (16–30 Hz), low-gamma (31–60 Hz), and high-gamma (61–120 Hz) bands (Hipp *et al.*, 2011; Haegens *et al.*, 2015). In the induced activity, sustained alpha and beta activities were particularly strong with additional multiple broadband induced gamma transients observed in the late window (Fig. 3C and F).

Frequency-specific response patterns in primary auditory cortex and posterior auditory field

Significant TFR responses at 6 dB above the site threshold were pooled for each group and the grand mean was determined. This level was chosen since here the level functions reached saturation (Supplementary Fig. 4A). At this stimulation level, the number of the responding sites in A1 and PAF were: in controls $n_{A1} = 236$ and $n_{PAF} = 166$ and in CDCs $n_{A1} = 119$ and $n_{PAF} = 184$. Corresponding to the individual examples, the evoked response (Fig. 4A, B, E and F) contained mainly activity within the early time window, while induced activity (Fig. 4C, D, G and H) contained both early and late activity.

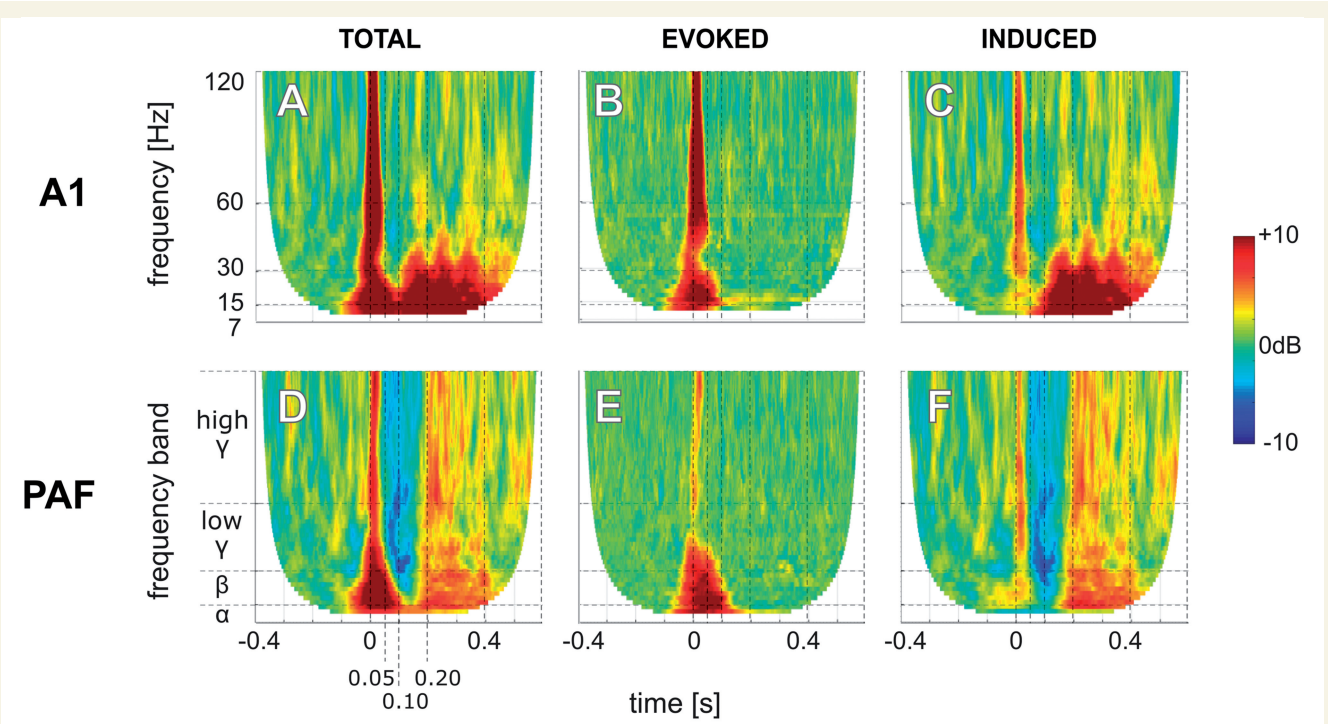

Figure 3 Time-frequency representation of the responses in an electrically-stimulated hearing control. TFRs of total (*left*, **A** and **D**), evoked (*middle*, **B** and **E**), and induced (*right*, **C** and **F**) responses in the primary A1 (*upper*, **A–C**) and the higher-order PAF (*lower*, **D–F**) from b-LFP signals in response to electric stimulation in a hearing control at the intensity of 6 dB above the site-threshold. Data are shown in decibel relative to the baseline (−400 ms to −100 ms prestimulus). Phase-locked evoked responses appear mainly at early latencies (< 100 ms) while the non-phase-locked induced responses appear dominantly at late latencies (> 100 ms).

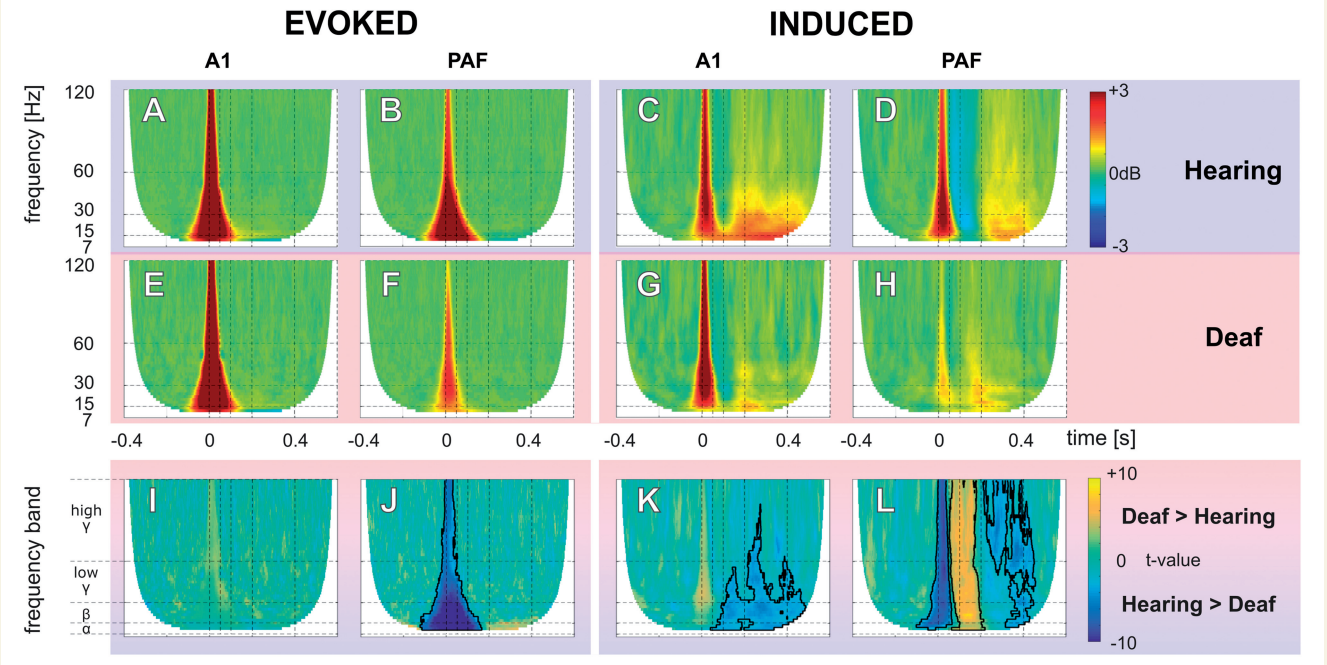

Figure 4 Grand mean and statistical comparison of evoked and induced TFR. (**A–H**) Grand mean of evoked (**A**, **B**, **E** and **F**), and induced (**C**, **D**, **G** and **H**) TFR responses from b-LFP in hearing electrically-stimulated controls (**A–D**), and CDCs (**E–H**) in field A1 and PAF. The evoked activity appeared at early-latency (< 100 ms), while the late-latency responses (> 100 ms) represent induced activity. All TFRs are shown in decibel relative to baseline (−400 ms to −100 ms prestimulus). (**I–L**) Results of non-parametric cluster-based permutation statistical testing (cluster α threshold 1%, two-tail significant α-value = 0.5%) for comparison between hearing and deaf animals. Data are shown in *t*-values, significant regions are outlined by black lines. (**I**) A1 evoked response comparison (**A** and **E**). (**J**) PAF evoked response comparison (**B** and **F**). (**K**) A1 induced response comparison (**C** and **G**). (**L**) PAF induced response comparison (**D** and **H**).

We observed spectral maxima in beta/low-gamma band in the early latency response and in alpha band in the late latency response (Supplementary Fig. 5). Additionally, in between early and late-latency response, a brief beta-gamma suppression (or desynchronization) of activity appeared (intermediate-latency responses in Supplementary Fig. 5), particularly strong in PAF of electrically-stimulated controls (Fig. 4D). This suppression was not observed in CDCs.

Comparing the evoked response, in A1 there was no significant difference between deaf and electrically-stimulated hearing animals (non-parametric cluster-based permutation analysis, Fig. 4I). However, in PAF, electrically-stimulated controls had stronger evoked responses than CDCs (area outlined by the black line in Fig. 4J). This may point to a stronger effect of congenital deafness on the secondary than the primary auditory cortex.

In the induced response, the differences between electrically-stimulated controls and CDCs were more pronounced. Here, the late response in CDCs was nearly lost in both A1 (Fig. 4K) and PAF (Fig. 4L). The only remaining portion of the late induced response in CDCs was found at its very beginning so that the weakening appeared to involve particularly the later portion of the induced responses. These pooled site-threshold aligned results also corresponded to the pooled 6 dB above E-ABR-threshold (Supplementary Fig. 6).

These results allow two conclusions: (i) in A1, there was no significant effect of deafness on the evoked responses, but a notable reduction of induced activity in all investigated frequencies (alpha, beta, gamma band). Consequently, evoked and induced responses can be functionally dissociated and appear to be differently affected by deafness in A1; and (ii) the adaptations to deafness were more extensive in PAF, which, while still being responsive to auditory stimulation, showed weaker responses both in the evoked and in the induced signals.

Effects of the stimulation mode

The above data compared electrically stimulated controls to electrically-stimulated CDCs; however, this comparison includes one confounding factor: the stimulation mode in controls. Electric stimulation is, in fact, an inadequate stimulus for hearing animals. We thus additionally compared the responses of acoustically stimulated to electrically-stimulated controls. Based on the level function, we decided to compare 40 dB acoustic stimulation to 6 dB electric stimulation (Supplementary Fig. 4). At this stimulation level, the number of resulting sites with significant responses in the acoustically-stimulated controls were $n_{A1} = 291$ and $n_{PAF} = 185$. In general, while providing similar results as for electric stimulation in controls, the induced PAF activity in acoustic stimulation (Fig. 5D) was even stronger when compared to the electric stimulation mode (Fig. 5H). This indicates that the differences

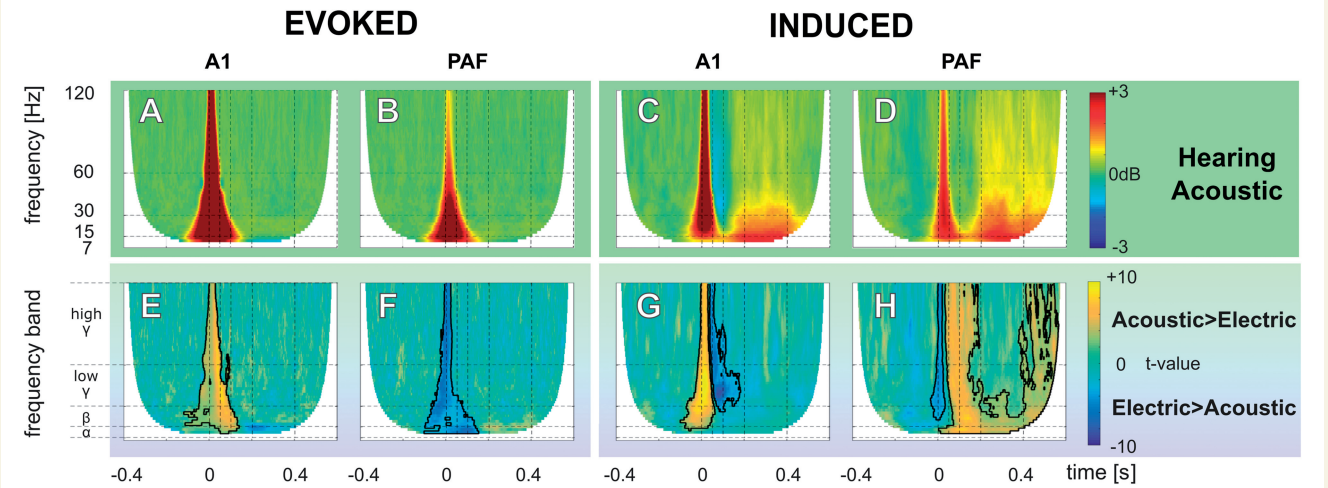

Figure 5 Grand mean and statistical comparison of evoked and induced TFR for acoustic stimulation. (**A–D**) Grand mean of evoked (**A** and **B**), and induced (**C** and **D**) TFR responses from b-LFP of acoustic-stimulated hearing controls in field A1 and PAF. All TFRs are shown in decibel relative to the baseline (−400 ms to −100 ms prestimulus). (**E–H**) Results of non-parametric cluster-based permutation statistical testing (cluster α threshold 1%, two-tail significant α-value = 0.5%) for the acoustic-stimulated and electrically-stimulated hearing groups comparison. (**E**) Evoked response comparison in A1 (**A** and Fig. 4A). (**F**) Evoked response comparison in PAF (**B** and Fig. 4B). (**G**) Induced response comparison in A1 (**C** and Fig. 4C). (**H**) Induced response comparison in PAF (**D** and Fig. 4D). Here, the induced late-latency activities in PAF were significantly stronger than in the hearing, acutely deafened animals.

between electrically-stimulated controls and CDCs actually underestimate the true difference.

Furthermore, we were curious whether the three groups of animals differed in the baseline. We computed power spectra from the subthreshold recordings for all groups (Fig. 6). Here the difference between groups was mainly observed in A1 (Fig. 6A): hearing animals with intact cochlea (green) had substantially more power in the ongoing activity compared to both the hearing, acutely deafened animals (blue) as well as the deaf animals (red). This indicates that the spontaneous activity in the auditory nerve, caused by intact hair cells, exerts a tonic drive on the ongoing activity in the primary fields in all bands, but most prominently in the alpha and beta range. The differences in ongoing activity were smaller in the secondary field PAF (Fig. 6D), corresponding to the weaker thalamic drive in the secondary fields. Importantly, in PAF the deaf animals showed significant reduction of ongoing alpha power while no significant difference was found between CDCs and acutely deafened controls in A1 (Fig. 6C). This may be related to cross-modal reorganization in PAF.

Discussion

The present study, to the best of our knowledge, for the first time demonstrates that the absence of experience preferentially affects induced responses. The induced response prominently differentiated hearing experienced animals from CDCs, both in the secondary and in the primary auditory cortex, and in all studied frequency bands (alpha, beta, and gamma). The present results thus demonstrate the differential role of developmental experience on evoked and induced activity. Cortical deficits in congenital deafness were more pronounced in the higher-order than primary sensory area.

The present data are consistent with previous analyses of evoked and induced responses in the auditory system with the similar structure of time-frequency responses (Delano *et al.*, 2008; Steinschneider *et al.*, 2008; Nourski *et al.*, 2014). While auditory evoked and induced response has been well described in normal hearing subjects (Tallon-Baudry and Bertrand, 1999; Trautner *et al.*, 2006; Fujioka *et al.*, 2009; Sedley *et al.*, 2016) and observed also in postlingual cochlear implant users (Agrawal *et al.*, 2013; Senkowski *et al.*, 2014), consequences of congenital deafness on this activity have remained unknown so far.

The functional role of induced activity

The functional role of induced responses has often been interpreted as reflecting 'top-down' modulation through backward connections (Engel *et al.*, 2001; Chen *et al.*, 2012; Morillon *et al.*, 2015) as opposed to the bottom-up driving processes that are more manifested in evoked components. The assumed role of induced responses is in feature-binding and top-down perceptual synthesis (Tallon-Baudry and Bertrand, 1999; Chen *et al.*, 2012). This concept is consistent with the observation that evoked activity dominates early-latency responses and appears as a brief transient, reflecting the brief thalamo-cortical input. Evoked responses are unlikely affected by other weak inputs (e.g. cortico-cortical). Induced activity additionally appeared at late-latencies and in a longer time window (similar as in Fründ *et al.*, 2008). Late-latency induced response, by its weaker coupling to the stimulus and long

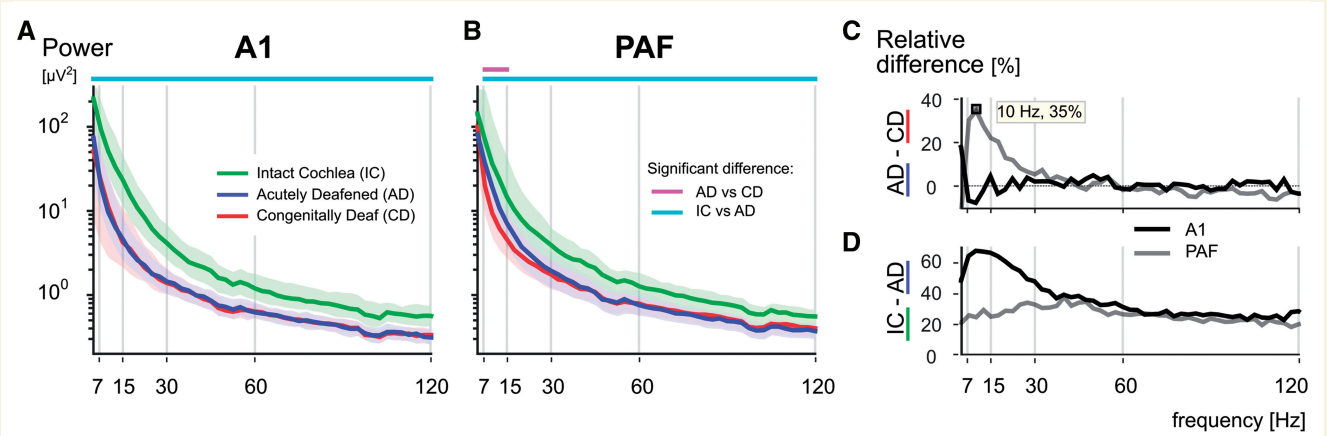

Figure 6 Power spectra of ongoing activity. (**A**) Grand median power spectra comparison of ongoing activity in hearing animals with intact cochlea (IC, green), hearing acutely deafened animals (AD, blue), and congenitally deaf animals (CD, red) for A1 (shaded areas representing the upper and lower quartiles). Statistical pair comparisons are shown for hearing versus deaf (magenta line above the graph) and animals with intact cochleae versus acutely deafened cochleae (cyan line above the graph) using two-tailed Wilcoxon rank-sum test (FDR corrected $q < 0.001$). Hearing animals with intact cochlea show significantly more power in the baseline throughout all frequencies than all other groups. (**B**) Same as (**A**) for PAF. (**C**) Relative difference in the power of ongoing activity between hearing acutely deafened and deaf animals, showing stronger alpha power (10 Hz peak) in hearing animals. Black line = A1; grey line = PAF. (**D**) Same as **C** between hearing animals with intact cochlea and those after acute deafening. More ongoing power was found in animals with intact cochleae throughout all frequencies, whereas in A1 it was most prominent in alpha and beta range. Black line = A1; grey line = PAF.

response duration, provides the possibility for its modification by weak cortico-cortical inputs originating from distant neuronal sources with delays caused by neuronal conduction from distant regions.

Synchrony in frequency-specific cortical activities may serve comparing the internal model with sensory inputs by the top-down interactions (Buzsáki and Chrobak, 1995; Engel *et al*., 2001). In an invasive study of hierarchical auditory cortical processing in normal hearing humans, gamma activity was more related to bottom-up, whereas low-frequency activity was more related to top-down information transfer (Fontolan *et al*., 2014). Similar results were obtained in the visual cortex of monkeys, where theta and gamma oscillations were related to the bottom-up and beta activity in the top-down information transfer (Bastos *et al*., 2015). In congenital deafness, a reduced top-down modulation of primary auditory cortex (its functional decoupling) has been suggested previously (Kral *et al*., 2005; Kral, 2013). All these studies are consistent with the present outcome of reduced induced signals in congenital deafness.

Though related to cognition, the induced gamma rhythm has also been reliably recorded in the anaesthetized animals previously (Logothetis *et al*., 2001; Brosch *et al*., 2002; Jia *et al*., 2011; Xing *et al*., 2012*b*). Anaesthesia may reduce responsiveness in higher-order areas (Sellers *et al*., 2015). This is, however, a function of the anaesthetic dose and regime. In the present study, the same anaesthetic regime was used in all groups of animals. We could reproducibly record induced activity in both investigated fields in all frequency bands in all animals, and the reported effects were specific to the deaf compared to hearing groups. Simultaneous recording further rules out anaesthesia as a reason for the differences between the fields. Though in the awake and attending condition, the induced activities have higher energy and better tuning (Xing *et al*., 2012*a*), we could reproducibly record them here. We expect higher induced energy in awake animals, particularly if engaged in a task.

The brain may determine the difference between the internal state (its prediction about the environment, the internal model) and the actual sensory input (Friston, 2010; Bastos *et al*., 2012). Such prediction error signal relates to learning in the adult brain, since it conveys information about the need to modify neuronal representations to better predict sensory inputs in the future. In the late-implanted congenitally deaf subjects plastic changes in neuronal processing were observed with experience, but they did not lead to adequate auditory performance even after years of experience (Schorr *et al*., 2005). The loss of induced signals observed here may explain this finding since it likely reflects the substantially decreased ability of the deaf cortex to integrate sensory input into ongoing cortico-cortical processing (*cf*. Engel *et al*., 2001; Morillon *et al*., 2015) and thus indicate the failure of generating error prediction signals required for the control of learning. The present data therefore help understanding why adult learning is ineffective in congenitally deaf late implanted subjects (Kral *et al*., 2017).

Reduced ongoing alpha power

In the ongoing activity we observed a reduced alpha power in PAF of CDCs corresponding to the findings in the visual system of subjects with neonatal cataracts (Bottari *et al*., 2016). The present study extends the previous result by

demonstrating that the effect is also observed in the auditory domain and that it can be localized to a higher-order sensory area. Alpha activity reflects the amount of functional suppression of neuronal resources not currently in use (Jensen and Mazaheri, 2010; Strauß *et al*., 2014). It is therefore interesting that in the absence of auditory experience alpha activity is downregulated—potentially to prevent the normal inhibition of PAF during visual stimulation and to allow gating cross-modal visual activity (Lomber *et al*., 2010) into higher brain structures. This is consistent with the absence of such effect in A1, where cross-modal reorganization was not observed (Kral *et al*., 2003; Lomber *et al*., 2010). Ongoing alpha activity may thus be a candidate of a functional fingerprint of cross-modal reorganization following deprivation.

Event-related desynchronization

Alpha/beta band suppression (or event-related desynchronization) during auditory stimulation has been described in scalp EEG (Pfurtscheller and Lopes da Silva, 1999; Fujioka and Ross, 2008; Leske *et al*., 2014; Senkowski *et al*., 2014), MEG (Todorovic *et al*., 2015), electrocorticography (ECoG) (Edwards *et al*., 2009; Pasley *et al*., 2012; de Pesters *et al*., 2016), and in intracortical recordings (Morillon *et al*., 2012; Fontolan *et al*., 2014), which appeared in relation to an increase of gamma activity. This suppression serves the function to increase the excitability in task-related cortical areas contrasted with task-unrelated areas (de Pesters *et al*., 2016). However, the majority of this evidence was with large-scale EEG recordings and the stimuli used in the above studies had long duration (>50 ms duration). In the present study, while some individual electrodes did reveal the same effect, such desynchronization was not consistent enough to show up in the grand mean. Potentially, the present stimuli were too short to induce the desynchronization (however, see Trautner *et al*., 2006). The use of local (spatially differentiated) signal additionally explains the absence of desynchronization in the grand mean data, similar to local TFR activities reported by the Lakatos and Schroeder labs (Lakatos *et al*., 2007; Haegens *et al*., 2015).

Higher-order cortical areas

Postnatal development of functional synapses in the primary auditory cortex is known to be regulated by hearing experience (Kral *et al*., 2005). While a number of deficits in feature sensitivity and cortical microcircuitry has been described in the primary auditory cortex of congenitally deaf animals, and their reversibility has been demonstrated with chronic cochlear implant electrostimulations (Kral *et al*., 2006), few information has so far been known about the higher-order auditory areas in congenital deafness.

Our results indicate that the higher-order area PAF shows more auditory deficits than the primary field A1 in congenital deafness. While A1 and PAF remain anatomically connected in CDCs (Barone *et al*., 2013; Butler *et al*., 2016), the anatomical cortico-cortical connectivity is likely not the same in detail when compared to hearing animals.

The deficits observed in the PAF were more extensive than in A1, but nevertheless, residual auditory-evoked activity was observed in PAF both in unit responses (Fig. 2) as well as in the evoked responses (Fig. 5). Thus, visual cross-modal reorganization in PAF (Lomber *et al*., 2010) does not eliminate auditory (evoked) responsiveness (for similar results in the dorsal auditory cortex, see Land *et al*., 2016). However, the specific power loss of ongoing alpha in PAF of deaf animals might be a signature of a switch from processing mainly auditory thalamic inputs towards processing new cortico-cortical (cross-modal) inputs. Alpha activity has a key role in both sensory processing (Haegens *et al*., 2015; Lakatos *et al*., 2016) as well as in gating cerebral activity, also between sensory systems (Jensen and Mazaheri, 2010). Alpha activity may also have a role in suppressing background noise from acoustic stimuli (Strauß *et al*., 2014; Dimitrijevic *et al*., 2017).

An event-related increase in synchronization of neuronal activity, as quantified by the PLF, can be interpreted as a phase-reset of the ongoing activity by an auditory stimulus (Lakatos *et al*., 2007, 2009, 2016; Mercier *et al*., 2015). In the present study, this phenomenon was affected by deafness only in PAF (Supplementary Fig. 4). From the standpoint of phase-locking to the auditory stimulus, it was again the higher-order field that showed a larger auditory deficit.

Developmental effects on oscillatory processes

There are few previous studies investigating the frequency-specific responses during auditory development. Throughout development, particularly during teenage years in humans, the energy in high-frequency oscillatory responses increases and the energy in low-frequency responses decreases with age (Uhlhaas *et al*., 2010; Fujioka *et al*., 2011; Cho *et al*., 2015). Furthermore, entrainment to sensory stimuli improves with age (Shahin *et al*., 2010). In the visual system, induced activity appeared only with increasing age (Uhlhaas *et al*., 2009). Using invasive recordings, cooing and babbling behaviour in children correlated with the appearance of high-frequency oscillatory activity (Cho-Hisamoto *et al*., 2012). A relation of the resting activity to performance has been suggested: the resting gamma activity predicts reading ability in teenagers (Tierney *et al*., 2014). Auditory training can further increase responses in the gamma range (Headley and Weinberger, 2011, 2013), which is further supported by more mature oscillatory and lateralized patterns in the experienced child's brain (Musacchia *et al*., 2017). Also, musicians show more induced responses than non-musicians (Trainor *et al*., 2009). These findings, together with the present results, suggest that development of brain rhythmic activity is regulated by sensory experience.

It is, therefore, tempting to speculate that the observed loss of induced activity is attributable to an arrested development of cortical circuits providing a neuronal substrate for generating the induced activity in the complete absence of sensory experience. Oscillatory activity, particularly for the high-frequency bands, reflects interactions between excitation and inhibition (Buzsáki and Wang, 2012). Previous studies documented a downregulation of inhibition in sensory deprivation as well as reduced temporal sensitivity of the inhibitory synapses in the auditory cortex (review in Sanes and Kotak, 2011). Such downregulated inhibition, reduced synchronization of cortical input (Hubka *et al*., 2005), and the pruning of too many synapses during development in deafness (Kral *et al*., 2005) may together contribute to the decrease in induced high-frequency activity in the deaf animals.

Conclusions

The present study provides evidence for a differential effect of early developmental experience on evoked and induced cortical activity. It implicates that cortico-cortical interactions are functionally more affected by the absence of hearing experience than thalamic inputs. Furthermore, several functional deficits were more extensively expressed in the higher-order than in the primary field, suggesting higher susceptibility of higher-order fields to the consequences of inborn deafness. Finally, the present study supports the concept that induced responses reflect previous experience and use of the given cortical region. Induced responses may potentially be used as a marker of a success after neurosensory restoration.

Acknowledgements

We thank Karl-Jürgen Kühne and Daniela Kühne for excellent help and assistance in the preparation and during the experiments, as well as preparing the histological data. P.A.Y. is on leave of absence from Dept. of Medical Physics, Faculty of Medicine, Universitas Indonesia and Biomedical Engineering Program, Faculty of Engineering, Universitas Indonesia.

Funding

Deutsche Forschungsgemeinschaft (DFG Kr 3370 and Exc 1077); MedEl Comp (to J.T.); DAAD – Indonesian German Scholarship Programme (IGSP) (50015396).

Supplementary material

Supplementary material is available at *Brain* online.

References

Agrawal D, Thorne JD, Viola FC, Timm L, Debener S, Büchner A, et al. Electrophysiological responses to emotional prosody perception in cochlear implant users. Neuroimage Clin 2013; 2: 229–38.

Alain C, Arnott SR, Picton TW. Bottom-up and top-down influences on auditory scene analysis: evidence from event-related brain potentials. J Exp Psychol Hum Percept Perform 2001; 27: 1072–89.

Arieli A, Sterkin A, Grinvald A, Aertsen A. Dynamics of ongoing activity: explanation of the large variability in evoked cortical responses. Science 1996; 273: 1868–71.

Barone P, Lacassagne L, Kral A. Reorganization of the connectivity of cortical field DZ in congenitally deaf cat. PLoS One 2013; 8: e60093.

Bastos AM, Schoffelen J. A tutorial review of functional connectivity analysis methods and their interpretational pitfalls. Front Syst Neurosci 2016; 9: 175.

Bastos AM, Usrey WM, Adams RA, Mangun GR, Fries P, Friston KJ. Canonical microcircuits for predictive coding. Neuron 2012; 76: 695–711.

Bastos AM, Vezoli J, Bosman CA, Schoffelen JM, Oostenveld R, Dowdall JR, et al. Visual areas exert feedforward and feedback influences through distinct frequency channels. Neuron 2015; 85: 390–401.

Benjamini Y, Yekutieli D. The control of the false discovery rate in multiple testing under dependency. Ann Stat 2001; 29: 1165–88.

Berkes P, Orban G, Lengyel M, Fiser J. Spontaneous cortical activity reveals hallmarks of an optimal internal model of the environment. Science 2011; 331: 83–7.

Bottari D, Troje NF, Ley P, Hense M, Kekunnaya R, Röder B. Sight restoration after congenital blindness does not reinstate alpha oscillatory activity in humans. Sci Rep 2016; 6: 24683.

Brosch M, Budinger E, Scheich H. Stimulus-related gamma oscillations in primate auditory cortex. J Neurophysiol 2002; 87: 2715–25.

Butler BE, Chabot N, Lomber SG. Quantifying and comparing the pattern of thalamic and cortical projections to the posterior auditory field in hearing and deaf cats. J Comp Neurol 2016; 524: 3042–63.

Buzsáki G, Chrobak JJ. Temporal structure in spatially organized neuronal ensembles: a role for interneuronal networks. Curr Opin Neurobiol 1995; 5: 504–10.

Buzsáki G, Wang XJ. Mechanisms of gamma oscillations. Annu Rev Neurosci 2012; 35: 203–25.

Castro-Alamancos MA. Dynamics of sensory thalamocortical synaptic networks during information processing states. Prog Neurobiol 2004; 74: 213–47.

Chen CC, Kiebel SJ, Kilner JM, Ward NS, Stephan KE, Wang WJ, et al. A dynamic causal model for evoked and induced responses. Neuroimage 2012; 59: 340–8.

Cho RY, Walker CP, Polizzotto NR, Wozny TA, Fissell C, Chen CM, et al. Development of sensory gamma oscillations and cross-frequency coupling from childhood to early adulthood. Cereb Cortex 2015; 25: 1509–18.

Cho-Hisamoto Y, Kojima K, Brown EC, Matsuzaki N, Asano E. Cooing- and babbling-related gamma-oscillations during infancy: intracranial recording. Epilepsy Behav 2012; 23: 494–6.

Cohen MX. Analyzing neural time series data: theory and practice. Massachusetts: The MIT Press; 2014.

David O, Kilner JM, Friston KJ. Mechanisms of evoked and induced responses in MEG/EEG. Neuroimage 2006; 31: 1580–91.

Delano PH, Pavez E, Robles L, Maldonado PE. Stimulus-dependent oscillations and evoked potentials in chinchilla auditory cortex. J Comp Physiol A Neuroethol Sens Neural Behav Physiol 2008; 194: 693–700.

Dimitrijevic A, Smith ML, Kadis DS, Moore DR. Cortical alpha oscillations predict speech intelligibility. Front Hum Neurosci 2017; 11: 88.

Donner TH, Siegel M. A framework for local cortical oscillation patterns. Trends Cogn Sci 2011; 15: 191–9.
Edgar JC, Khan SY, Blaskey L, Chow VY, Rey M, Gaetz W, et al. Neuromagnetic oscillations predict evoked-response latency delays and core language deficits in autism spectrum disorders. J Autism Dev Disord 2015; 45: 395–405.
Edwards E, Soltani M, Kim W, Dalal SS, Nagarajan SS, Berger MS, et al. Comparison of time-frequency responses and the event-related potential to auditory speech stimuli in human cortex. J Neurophysiol 2009; 102: 377–86.
Eggermont JJ. Stimulus induced and spontaneous rhythmic firing of single units in cat primary auditory cortex. Hear Res 1992; 61: 1–11.
Engel AK, Fries P, Singer W. Dynamic predictions: oscillations and synchrony in top-down processing. Nat Rev Neurosci 2001; 2: 704–16.
Fallon JB, Shepherd RK, Nayagam DA, Wise AK, Heffer LF, Landry TG, et al. Effects of deafness and cochlear implant use on temporal response characteristics in cat primary auditory cortex. Hear Res 2014; 315: 1–9.
Fiebelkorn IC, Snyder AC, Mercier MR, Butler JS, Molholm S, Foxe JJ. Cortical cross-frequency coupling predicts perceptual outcomes. Neuroimage 2013; 69: 126–37.
Fontolan L, Morillon B, Liegeois-Chauvel C, Giraud AL. The contribution of frequency-specific activity to hierarchical information processing in the human auditory cortex. Nat Commun 2014; 5: 4694.
Friston K. The free-energy principle: a unified brain theory? Nat Rev Neurosci 2010; 11: 127–38.
Fründ I, Busch NA, Schadow J, Gruber T, Körner U, Herrmann CS. Time pressure modulates electrophysiological correlates of early visual processing. PLoS One 2008; 3: e1675.
Fujioka T, Mourad N, Trainor LJ. Development of auditory-specific brain rhythm in infants. Eur J Neurosci 2011; 33: 521–9.
Fujioka T, Ross B. Auditory processing indexed by stimulus-induced alpha desynchronization in children. Int J Psychophysiol 2008; 68: 130–40.
Fujioka T, Trainor LJ, Large EW, Ross B. Beta and gamma rhythms in human auditory cortex during musical beat processing. Ann N Y Acad Sci 2009; 1169: 89–92.
Gandal MJ, Edgar JC, Ehrlichman RS, Mehta M, Roberts TP, Siegel SJ. Validating γ oscillations and delayed auditory responses as translational biomarkers of autism. Biol Psychiatry 2010; 68: 1100–6.
Gilbert CD, Sigman M. Brain states: top-down influences in sensory processing. Neuron 2007; 54: 677–96.
Giraud AL, Poeppel D. Cortical oscillations and speech processing: emerging computational principles and operations. Nat Neurosci 2012; 15: 511–17.
Goswami U. A temporal sampling framework for developmental dyslexia. Trends Cogn Sci 2011; 15: 3–10.
Goswami U. Sensory theories of developmental dyslexia: three challenges for research. Nat Rev Neurosci 2014; 16: 43–54.
Griffiths TD, Kumar S, Sedley W, Nourski KV, Kawasaki H, Oya H, et al. Direct recordings of pitch responses from human auditory cortex. Curr Biol 2010; 20: 1128–32.
Haegens S, Barczak A, Musacchia G, Lipton ML, Mehta AD, Lakatos P, et al. Laminar profile and physiology of the α rhythm in primary visual, auditory, and somatosensory regions of neocortex. J Neurosci 2015; 35: 14341–52.
Handa T, Takekawa T, Harukuni R, Isomura Y, Fukai T. Medial frontal circuit dynamics represents probabilistic choices for unfamiliar sensory experience. Cereb Cortex 2017; 27: 3818–31.
Hartmann R, Topp G, Klinke R. Discharge patterns of cat primary auditory fibers with electrical stimulation of the cochlea. Hear Res 1984; 13: 47–62.
Headley DB, Weinberger NM. Gamma-band activation predicts both associative memory and cortical plasticity. J Neurosci 2011; 31: 12748–58.
Headley DB, Weinberger NM. Fear conditioning enhances γ oscillations and their entrainment of neurons representing the conditioned stimulus. J Neurosci 2013; 33: 5705–17.
Heid S, Hartmann R, Klinke R. A model for prelingual deafness, the congenitally deaf white cat–population statistics and degenerative changes. Hear Res 1998; 115: 101–12.
Heim S, Friedman JT, Keil A, Benasich AA. Reduced sensory oscillatory activity during rapid auditory processing as a correlate of language-learning impairment. J Neurolinguistics 2011; 24: 538–55.
Herrmann CS, Rach S, Vosskuhl J, Strüber D. Time–frequency analysis of event-related potentials: a brief tutorial. Brain Topogr 2014; 27: 438–50.
Hipp JF, Engel AK, Siegel M. Oscillatory synchronization in large-scale cortical networks predicts perception. Neuron 2011; 69: 387–96.
Hubka P, Kral A, Klinke R. Input desynchronization and impaired columnar activation in deprived auditory cortex revealed by independent component analysis. In: Syka J, Merzenich MM, editors. Plasticity and signal representation in the auditory system. Boston, MA: Springer US; 2005. p. 191–5.
Ito M. Control of mental activities by internal models in the cerebellum. Nat Rev Neurosci 2008; 9: 304–13.
Jensen O, Mazaheri A. Shaping functional architecture by oscillatory alpha activity: gating by inhibition. Front Hum Neurosci 2010; 4: 186.
Jia X, Smith MA, Kohn A. Stimulus selectivity and spatial coherence of gamma components of the local field potential. J Neurosci 2011; 31: 9390–403.
Kral A. Auditory critical periods: a review from system's perspective. Neuroscience 2013; 247: 117–33.
Kral A, Eggermont JJ. What's to lose and what's to learn: development under auditory deprivation, cochlear implants and limits of cortical plasticity. Brain Res Rev 2007; 56: 259–69.
Kral A, Hubka P, Heid S, Tillein J. Single-sided deafness leads to unilateral aural preference within an early sensitive period. Brain 2013; 136: 180–93.
Kral A, Lomber SG. Deaf white cats. Curr Biol 2015; 25: R351–3.
Kral A, Schröder JH, Klinke R, Engel AK. Absence of cross-modal reorganization in the primary auditory cortex of congenitally deaf cats. Exp Brain Res 2003; 153: 605–13.
Kral A, Tillein J, Hartmann R, Klinke R. Monitoring of anaesthesia in neurophysiological experiments. Neuroreport 1999; 10: 781–7.
Kral A, Tillein J, Heid S, Hartmann R, Klinke R. Postnatal cortical development in congenital auditory deprivation. Cereb Cortex 2005; 15: 552–62.
Kral A, Tillein J, Heid S, Klinke R, Hartmann R. Cochlear implants: cortical plasticity in congenital deprivation. Prog Brain Res 2006; 157: 283–313.
Kral A, Tillein J, Hubka P, Schiemann D, Heid S, Hartmann R, et al. Spatiotemporal patterns of cortical activity with bilateral cochlear implants in congenital deafness. J Neurosci 2009; 29: 811–27.
Kral A, Yusuf PA, Land R. Higher-order auditory areas in congenital deafness: top-down interactions and corticocortical decoupling. Hear Res 2017; 343: 50–63.
Lakatos P, Barczak A, Neymotin SA, McGinnis T, Ross D, Javitt DC, et al. Global dynamics of selective attention and its lapses in primary auditory cortex. Nat Neurosci 2016; 19: 1707–17.
Lakatos P, Chen CM, O'Connell MN, Mills A, Schroeder CE. Neuronal oscillations and multisensory interaction in primary auditory cortex. Neuron 2007; 53: 279–92.
Lakatos P, O'Connell MN, Barczak A, Mills A, Javitt DC, Schroeder CE. The leading sense: supramodal control of neurophysiological context by attention. Neuron 2009; 64: 419–30.
Land R, Baumhoff P, Tillein J, Lomber SG, Hubka P, Kral A. Cross-modal plasticity in higher-order auditory cortex of congenitally deaf cats does not limit auditory responsiveness to cochlear implants. J Neurosci 2016; 36: 6175–85.
Land R, Engler G, Kral A, Engel AK. Auditory evoked bursts in mouse visual cortex during isoflurane anesthesia. PLoS One 2012; 7: e49855.
Leske S, Tse A, Oosterhof NN, Hartmann T, Müller N, Keil J, et al. The strength of alpha and beta oscillations parametrically scale with the strength of an illusory auditory percept. Neuroimage 2014; 88: 69–78.

Lewis AG, Wang L, Bastiaansen M. Fast oscillatory dynamics during language comprehension: unification versus maintenance and prediction? Brain Lang 2015a; 148: 51–63.
Lewis LD, Voigts J, Flores FJ, Schmitt LI, Wilson MA, Halassa MM, et al. Thalamic reticular nucleus induces fast and local modulation of arousal state. Elife 2015b; 4: e08760.
Logothetis NK, Pauls J, Augath M, Trinath T, Oeltermann A. Neurophysiological investigation of the basis of the fMRI signal. Nature 2001; 412: 150–7.
Lomber SG, Meredith MA, Kral A. Cross-modal plasticity in specific auditory cortices underlies visual compensations in the deaf. Nat Neurosci 2010; 13: 1421–7.
Maris E, Oostenveld R. Nonparametric statistical testing of EEG- and MEG-data. J Neurosci Methods 2007; 164: 177–90.
McMains S, Kastner S. Interactions of top-down and bottom-up mechanisms in human visual cortex. J Neurosci 2011; 31: 587–97.
Mercier MR, Molholm S, Fiebelkorn IC, Butler JS, Schwartz TH, Foxe JJ. Neuro-oscillatory phase alignment drives speeded multisensory response times: an electro-corticographic investigation. J Neurosci 2015; 35: 8546–57.
Morillon B, Hackett TA, Kajikawa Y, Schroeder CE. Predictive motor control of sensory dynamics in auditory active sensing. Curr Opin Neurobiol 2015; 31: 230–8.
Morillon B, Liégeois-Chauvel C, Arnal LH, Bénar CG, Giraud AL. Asymmetric function of theta and gamma activity in syllable processing: an intra-cortical study. Front Psychol 2012; 3: 248.
Murphy E, Benítez-Burraco A. Language deficits in schizophrenia and autism as related oscillatory connectomopathies: an evolutionary account. Neurosci Biobehav Rev 2017. doi: 10.1016/j.neubiorev.2016.07.029.
Musacchia G, Ortiz-Mantilla S, Choudhury N, Realpe-Bonilla T, Roesler C, Benasich AA. Active auditory experience in infancy promotes brain plasticity in theta and gamma oscillations. Dev Cogn Neurosci 2017; 26: 9–19.
van de Nieuwenhuijzen ME, Axmacher N, Fell J, Oehrn CR, Jensen O, van Gerven MAJ. Decoding of task-relevant and task-irrelevant intracranial EEG representations. Neuroimage 2016; 137: 132–9.
Nourski KV, Steinschneider M, Oya H, Kawasaki H, Jones RD, Howard MA. Spectral organization of the human lateral superior temporal gyrus revealed by intracranial recordings. Cereb Cortex 2014; 24: 340–52.
Oostenveld R, Fries P, Maris E, Schoffelen JM. FieldTrip: open source software for advanced analysis of MEG, EEG, and invasive electrophysiological data. Comput Intell Neurosci 2011; 2011: 156869.
Pasley BN, David SV, Mesgarani N, Flinker A, Shamma SA, Crone NE, et al. Reconstructing speech from human auditory cortex. PLoS Biol 2012; 10: e1001251.
de Pesters A, Coon WG, Brunner P, Gunduz A, Ritaccio AL, Brunet NM, et al. Alpha power indexes task-related networks on large and small scales: a multimodal ECoG study in humans and a non-human primate. Neuroimage 2016; 134: 122–31.
Pfurtscheller G, Lopes da Silva FH. Event-related EEG/MEG synchronization and desynchronization: basic principles. Clin Neurophysiol 1999; 110: 1842–57.
Poulet JF, Petersen CC. Internal brain state regulates membrane potential synchrony in barrel cortex of behaving mice. Nature 2008; 454: 881–5.
Quiroga RQ, Nadasdy Z, Ben-Shaul Y. Unsupervised spike detection and sorting with wavelets and superparamagnetic clustering. Neural Comput 2004; 16: 1661–87.
Riecke L, Sack AT, Schroeder CE. Endogenous delta/theta sound-brain phase entrainment accelerates the buildup of auditory streaming. Curr Biol 2015; 25: 3196–201.
Ross B, Barat M, Fujioka T. Sound-making actions lead to immediate plastic changes of neuromagnetic evoked responses and induced β-band oscillations during perception. J Neurosci 2017; 37: 5948–59.
Sanes DH, Kotak VC. Developmental plasticity of auditory cortical inhibitory synapses. Hear Res 2011; 279: 140–8.
Schorr EA, Fox NA, van Wassenhove V, Knudsen EI. Auditory-visual fusion in speech perception in children with cochlear implants. Proc Natl Acad Sci USA 2005; 102: 18748–50.
Sedley W, Gander PE, Kumar S, Kovach CK, Oya H, Kawasaki H, et al. Neural signatures of perceptual inference. Elife 2016; 5: e11476.
Sellers KK, Bennett DV, Hutt A, Williams JH, Fröhlich F. Awake vs. anesthetized: layer-specific sensory processing in visual cortex and functional connectivity between cortical areas. J Neurophysiol 2015; 113: 3798–815.
Senkowski D, Pomper U, Fitzner I, Engel AK, Kral A. Beta-band activity in auditory pathways reflects speech localization and recognition in bilateral cochlear implant users. Hum Brain Mapp 2014; 35: 3107–21.
Shahin AJ, Picton TW, Miller LM. Brain oscillations during semantic evaluation of speech. Brain Cogn 2009; 70: 259–66.
Shahin AJ, Trainor LJ, Roberts LE, Backer KC, Miller LM. Development of auditory phase-locked activity for music sounds. J Neurophysiol 2010; 103: 218–29.
Steinschneider M, Fishman YI, Arezzo JC. Spectrotemporal analysis of evoked and induced electroencephalographic responses in primary auditory cortex (A1) of the awake monkey. Cereb Cortex 2008; 18: 610–25.
Steriade M. Central core modulation of spontaneous oscillations and sensory transmission in thalamocortical systems. Curr Opin Neurobiol 1993; 3: 619–25.
Strauß A, Wöstmann M, Obleser J. Cortical alpha oscillations as a tool for auditory selective inhibition. Front Hum Neurosci 2014; 8: 350.
Tallon-Baudry C, Bertrand O. Oscillatory gamma activity in humans and its role in object representation. Trends Cogn Sci 1999; 3: 151–62.
Tallon-Baudry C, Bertrand O, Delpuech C, Pernier J. Stimulus specificity of phase-locked and non-phase-locked 40 Hz visual responses in human. J Neurosci 1996; 16: 4240–9.
Tierney A, Strait DL, Kraus N. Resting gamma power is linked to reading ability in adolescents. Dev Sci 2014; 17: 86–93.
Tillein J, Hubka P, Kral A. Monaural congenital deafness affects aural dominance and degrades binaural processing. Cereb Cortex 2016; 26: 1762–77.
Tillein J, Hubka P, Syed E, Hartmann R, Engel AK, Kral A. Cortical representation of interaural time difference in congenital deafness. Cereb Cortex 2010; 20: 492–506.
Todorovic A, Schoffelen JM, van Ede F, Maris E, de Lange FP. Temporal expectation and attention jointly modulate auditory oscillatory activity in the beta band. PLoS One 2015; 10: e0120288.
Trainor LJ, Shahin AJ, Roberts LE. Understanding the benefits of musical training: effects on oscillatory brain activity. Ann N Y Acad Sci 2009; 1169: 133–42.
Trautner P, Rosburg T, Dietl T, Fell J, Korzyukov OA, Kurthen M, et al. Sensory gating of auditory evoked and induced gamma band activity in intracranial recordings. Neuroimage 2006; 32: 790–8.
Uhlhaas PJ, Roux F, Rodriguez E, Rotarska-Jagiela A, Singer W. Neural synchrony and the development of cortical networks. Trends Cogn Sci 2010; 14: 72–80.
Uhlhaas PJ, Roux F, Singer W, Haenschel C, Sireteanu R, Rodriguez E. The development of neural synchrony reflects late maturation and restructuring of functional networks in humans. Proc Natl Acad Sci USA 2009; 106: 9866–71.
Wolpert DM, Ghahramani Z, Jordan MI. An internal model for sensorimotor integration. Science 1995; 269: 1880–2.
Wöstmann M, Lim SJ, Obleser J. The human neural alpha response to speech is a proxy of attentional control. Cereb Cortex 2017; 27: 3307–17.
Xing D, Shen Y, Burns S, Yeh CI, Shapley RM, Li W. Stochastic generation of gamma-band activity in primary visual cortex of awake and anesthetized monkeys. J Neurosci 2012a; 32: 13873–80a.
Xing D, Yeh CI, Burns S, Shapley RM. Laminar analysis of visually evoked activity in the primary visual cortex. Proc Natl Acad Sci USA 2012b; 109: 13871–6.